Supplement of Biogeosciences, 12, 3973–3992, 2015
http://www.biogeosciences.net/12/3973/2015/
doi:10.5194/bg-12-3973-2015-supplement
© Author(s) 2015. CC Attribution 3.0 License.

Biogeosciences
Open Access

Supplement of

Changes in dissolved iron deposition to the oceans driven by human activity: a 3-D global modelling study

S. Myriokefalitakis et al.

Correspondence to: S. Myriokefalitakis (stelios@uoc.gr) and M. Kanakidou (mariak@uoc.gr)

The copyright of individual parts of the supplement might differ from the CC-BY 3.0 licence.

Table S1. Emissions used in TM4-ECPL for PRESENT (year 2008), PAST (year 1850) and FUTURE (year 2100) simulations**.** All emissions are in Tg yr^{-1}, except for NOx (Tg-N yr^{-1}), NH_3 (Tg-N yr^{-1}), SO_x (Tg-S yr^{-1}) and DMS (Tg-S yr^{-1}).

Species	Year	Biomass Burning	Anthropogenic	Aircrafts	Ships	Biogenic	Soils	Oceans
ACETONE	1850	6.46E-02	4.23E-01			3.59E+01		
	2008	4.23E+00	2.64E+00	3.03E-07				
	2100	5.09E+00	2.73E+00	2.80E-07				
BC	1850	2.62E-01	1.05E+00		8.05E-04			
	2008	2.62E+00	5.39E+00	8.39E-06	1.24E-01			
	2100	3.17E+00	1.11E+00	7.32E-06	1.43E-02			
BENZENE	1850	4.83E-01	7.51E-01		8.05E-04			
	2008	4.83E+00	6.31E+00	4.90E-06	1.16E-01			
	2100	5.89E+00	2.15E+00	4.52E-06	4.80E-02			
C_2H_4	1850	6.35E-01	1.24E+00		2.21E-03	1.75E+01		1.20E+00
	2008	6.35E+00	6.87E+00	3.04E-06	2.57E-01			
	2100	7.76E+00	2.24E+00	2.80E-06	1.06E-01			
C_2H_6	1850	3.17E-01	5.93E-01		1.01E-03	3.01E-01		8.00E-01
	2008	3.17E+00	2.87E+00	4.37E-06	1.50E-01			
	2100	3.96E+00	8.09E-01	4.03E-06	6.22E-02			
C_3H_6	1850	6.26E-01	9.14E-01		2.56E-03	1.66E+01		1.30E+00
	2008	6.25E+00	6.41E+00	4.64E-06	2.98E-01			
	2100	7.68E+00	2.27E+00	4.29E-06	1.23E-01			
C_3H_8	1850	1.96E-01	2.42E-01		1.96E-01	3.01E-02		1.00E+00
	2008	1.96E+00	3.47E+00	4.87E-06	4.17E-01			
	2100	2.54E+00	1.26E+00	4.50E-06	1.73E-01			
C_4H_{10}	1850	9.07E-02	4.56E-01		6.27E-03	6.09E-02		6.80E+00
	2008	9.07E-01	3.32E+01	4.01E-05	8.79E-01			
	2100	1.11E+00	1.96E+01	3.70E-05	3.64E-01			
CH_2O	1850	5.87E-01	1.45E-01			4.33E+00		
	2008	5.86E+00	3.39E+00	7.54E-07				
	2100	7.21E+00	1.43E+00	6.97E-07				
CH_3CHO	1850	4.86E-01	3.16E-01			2.04E+01		
	2008	4.85E+00	1.80E+00	2.07E-06				
	2100	6.00E+00	5.95E-01	1.91E-06				
CH_3OH	1850	1.17E+00	6.14E-01			1.38E+02		
	2008	1.17E+01	4.87E+00	2.90E-06				
	2100	1.42E+01	2.85E+00	2.68E-06				

CO	1850	4.61E+01	6.30E+01		7.74E-03	8.37E+01		2.00E+01
	2008	4.60E+02	5.99E+02	6.55E-04	1.15E+00			
	2100	5.49E+02	2.34E+02	5.11E-04	2.29E-01			
MEK	1850	0.00E+00	0.00E+00	0.00E+00	0.00E+00	6.98E-01		
	2008			1.04E-06				
	2100			9.58E-07				
NOx	1850	7.74E-03	7.74E-03		7.74E-03		8.00E+00	
	2008	5.48E+00	2.67E+01	1.44E-03	5.14E+00			
	2100	6.39E+00	7.48E+00	1.84E-03	9.47E-01			
POA	1850	2.33E+00	4.63E+00		9.05E-04			
	2008	2.33E+01	1.39E+01	2.52E-06	1.29E-01			
	2100	2.82E+01	3.46E+00	2.20E-06	1.42E-02			
SOx	1850	1.93E-01	1.01E+00		3.60E-02			
	2008	1.93E+00	4.69E+01	1.14E-04	5.22E+00			
	2100	2.21E+00	7.70E+00	1.00E-04	5.04E-01			
TOLUENE	1850	1.42E-01	3.55E-01		5.71E-04	1.41E+00		
	2008	1.42E+00	7.22E+00	7.36E-06	6.71E-02			
	2100	1.73E+00	4.70E+00	6.80E-06	2.78E-02			
XYLENE	1850	3.71E-02	2.57E-01		1.56E-03			
	2008	3.70E-01	1.18E+01	6.69E-06	2.06E-01			
	2100	4.51E-01	7.66E+00	8.52E-02	6.18E-06			
CH_3COOH	1850	1.73E+00	1.45E+00			3.25E+00		
	2008	1.73E+01	7.46E+00					
	2100	2.08E+01	2.33E+00					
HCOOH	1850	4.33E-01	3.62E-01			3.25E+00		
	2008	4.32E+00	1.87E+00					
	2100	5.21E+00	5.83E-01					
DMS	1850	1.47E-04						1.90E+01
	2008	1.47E-03						
	2100	1.76E-03						
GLY	1850	5.87E-01						2.00E+01
	2008	5.86E+00						
	2100	7.21E+00						
NH3	1850	9.20E-01	5.40E+00					8.00E+00
	2008	9.20E+00	3.41E+01					
	2100	1.00E+01	5.15E+01					
ISOPRENE	2008					5.20E+02		1.00E+00
TERPENE	2008					1.04E+02		2.00E-04

Table S2. Aqueous-phase mechanism for Fe chemistry used in the TM4-ECPL model.

Reactions	K_{298} ($M^{-n+1}s^{-1}$)	Ea/R (K)	References
$Fe^{2+} + H_2O_2 \rightarrow Fe^{3+} + OH + {}^{-}OH$	5.24×10^{1}	5050	Kremer, 2003
$Fe^{2+} + O_2^{-\cdot} + 2H^{+} \rightarrow Fe^{3+} + H_2O_2$	1.00×10^{7}	5050	Rush and Bielski, 1985
$Fe^{2+} + HO_2 + H^{+} \rightarrow Fe^{3+} + H_2O_2$	1.20×10^{6}	5050	Jayson et al., 1973b
$Fe^{2+} + OH \rightarrow Fe(OH)^{2+}$	4.60×10^{8}	1100	Christensen and Sehested, 1981
$Fe^{2+} + NO_3 \rightarrow Fe^{3+} + NO_3^{-}$	8.00×10^{6}		Pikaev et al., 1974
$Fe^{2+} + NO_2 + H+ \rightarrow Fe^{3+} + HONO$	3.10×10^{4}		Epstein et al., 1982
$Fe^{2+} + O_3$ (+ H_2O) $\rightarrow Fe(OH)^{2+} + OH + O_2$ (*)	8.20×10^{5}		Logager et al., 1992
$Fe^{3+} + hv$ (+ H_2O) $\rightarrow Fe^{2+} + OH + H^{+}$	$6.41 \text{ x } 10^{-6}$		Benkelberg and Warneck, 1995
$Fe(OH)^{2+} + hv \rightarrow Fe^{2+} + OH$	4.51×10^{-3}		Benkelberg and Warneck, 1995
$Fe(OH)_2^{+} + hv \rightarrow Fe^{2+} + OH + {}^{-}OH$	5.77×10^{-3}		Benkelberg et al., 1991
$Fe(OH)^{2+} + O_2^{-} \rightarrow Fe^{2+} + O_2 + {}^{-}OH$	1.50×10^{8}		Rush and Bielski, 1985
$Fe(OH)^{2+} + HO_2 \rightarrow Fe^{2+} + O_2 + H_2O$	1.30×10^{5}		Ziajka et al., 1994
$Fe^{3+} + SO_4^{2-} \rightarrow Fe(SO_4)^{+}$	3.20×10^{3}		Jayson et al., 1973b
$Fe(SO_4)^{+} \rightarrow Fe^{3+} + SO_4^{2-}$	2.70×10^{1}		Jayson et al., 1973b
$Fe(SO_4)^{+} + hv \rightarrow Fe^{2+} + SO_4^{-}$	6.43×10^{-3}		Lin et al., 2014
$Fe^{3+} + C_2O_4^{2-} \rightarrow Fe(C_2O_4)^{+}$	7.50×10^{6}		Lin et al., 2014
$Fe(C_2O_4)^{+} \rightarrow Fe^{3+} + C_2O_4^{2-}$	3.00×10^{-3}		Lin et al., 2014
$Fe(C_2O_4)^{+} + C_2O_4^{2-} \rightarrow Fe(C_2O_4)_2^{-}$	1.89×10^{4}		Lin et al., 2014
$Fe(C_2O_4)_2^{-} \rightarrow Fe(C_2O_4)^{+} + C_2O_4^{2-}$	3.30×10^{-3}		Lin et al., 2014
$Fe(C_2O_4)^{+} + O_2^{-} \rightarrow Fe(C_2O_4) + O_2$	1.00×10^{6}		Sedlak and Hoigne, 1993
$Fe(C_2O_4)^{+} + HO_2 \rightarrow Fe(C_2O_4) + O_2 + H^{+}$	1.20×10^{5}		Sedlak and Hoigne, 1993
$Fe(C_2O_4)_2^{-} + O_2^{-} \rightarrow Fe(C_2O_4)_2^{2-} + O_2$	1.00×10^{6}		Sedlak and Hoigne, 1993
$Fe(C_2O_4)_2^{-} + HO_2 \rightarrow Fe(C_2O_4)_2^{2-} + O_2 + H^{+}$	1.20×10^{5}		Sedlak and Hoigne, 1993
$Fe(C_2O_4) + H_2O_2 \rightarrow Fe(C_2O_4)^{+} + OH + {}^{-}OH$	5.24×10^{4}		Sedlak and Hoigne, 1993
$Fe(C_2O_4)_2^{-} + hv$ (+ O_2) $\rightarrow Fe^{+2} + C_2O_4^{2-} + 2CO_2 + O_2^{-}$	2.47×10^{-2}		Lin et al., 2014
Equilibrium	Keq (mol kg^{-1})		References
$Fe^{3+} + H_2O \leftrightarrow Fe(OH)^{2+} + H^{+}$	1.10×10^{-4}		Ervens et al., 2003
$Fe(OH)^{2+} + H_2O \leftrightarrow Fe(OH)_2^{+} + H^{+}$	1.40×10^{-7}		Ervens et al., 2003

(*) For simplicity FeO^{2+} formation is neglected and formation of $Fe(OH)^{2+}$ is here considered.

Table S3. Number of measurements (N), mean correlation coefficient (*r*), normalised mean bias (*NMB*), normalised mean error (*NME*) and root mean square error (*RMSE*) values calculated for total Iron (TFe) and dissolved Iron (DFe) as presented in Figure 5.

Figure	Observations	N	R	NMB (%)	NME (%)	RMSE
Fig. 5a	**TFe (ng-Fe m^{-3})**	412	0.07	37	147	619
Fig. 5b	**DFe (ng-Fe m^{-3})**	412	0.07	67	84	29
Fig. 5c	**SFe (%)**	412	0.07	47	20	174
Fig. 5d	**TFe (ng-Fe m^{-3})**	452	0.4	-26	82	77
Fig. S5i	**OXL-with Fe-Oxalato Chemistry (ng m^{-3})**	130	0.47	-0.396	69	233
Fig. S5i	**OXL-without Fe-Oxalato Chemistry (ng m^{-3})**	130	0.47	2.110	68	231

$$R = \left[\frac{\frac{1}{N}\sum_{i=1}^{N}\left(O_i - \overline{O}\right)\left(P_i - \overline{P}\right)}{\sigma_O \sigma_P} \right] \qquad \text{(eq. S1)}$$

$$NMB = \frac{\sum_{i=1}^{N}\left(M_i - O_i\right)}{\sum_{i=1}^{N} O_i} \times 100 \qquad \text{(eq. S2)}$$

$$RMSE = \sqrt{\frac{1}{N}\sum_{i=1}^{N}\left(P_i - O_i\right)^2} \qquad \text{(eq. S3)}$$

$$NME = \frac{\sum_{i=1}^{N}\left|M_i - O_i\right|}{\sum_{i=1}^{N} O_i} \times 100 \qquad \text{(eq. S4)}$$

Figure S1. Annual emissions (ng m^{-2} s^{-1}) as taken into account by TM4-ECPL for the present atmosphere of a) dust and of Fe contained in: b) kaolinite, c) illite, d) smectite, e) hematite, f) feldspars g) in fossil fuels (including shipping oil combustion aerosols) and h) in biomass burning aerosols.

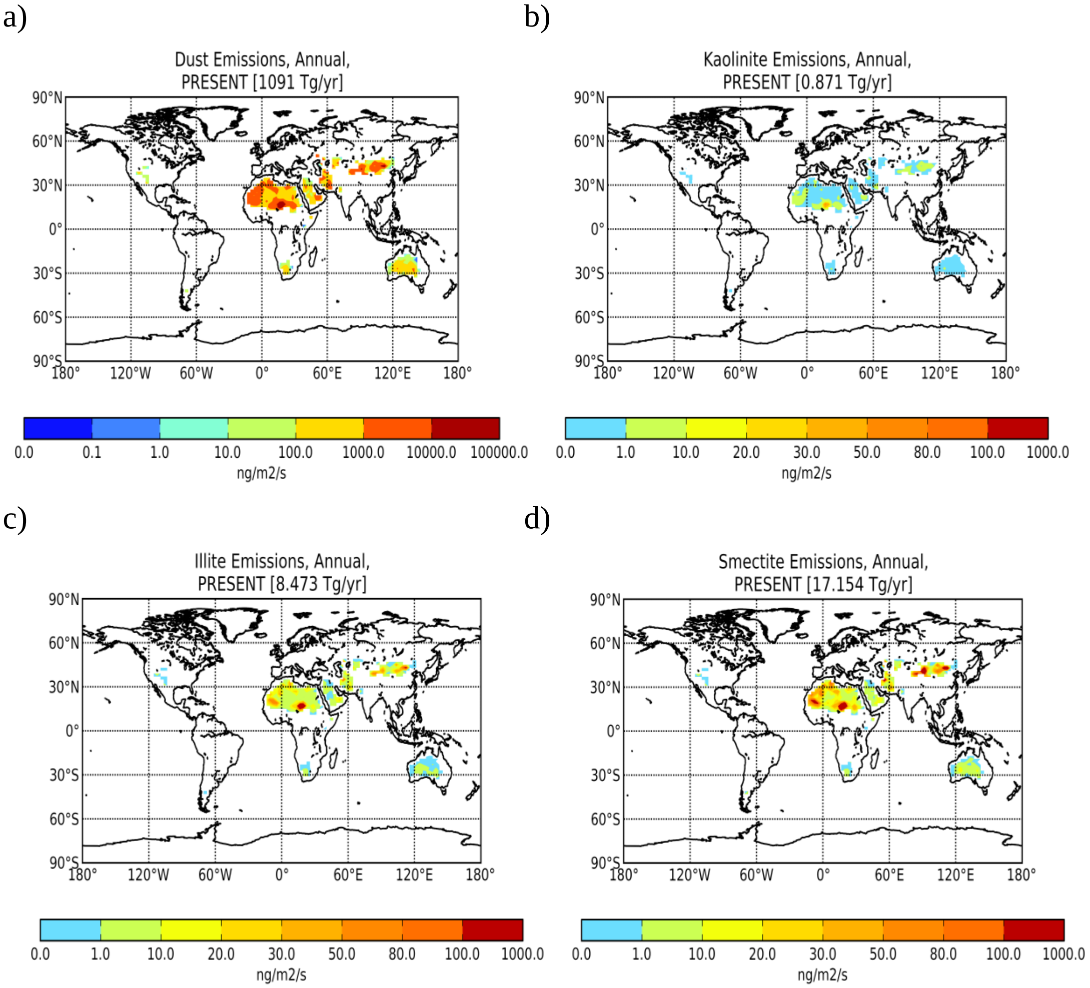

e)

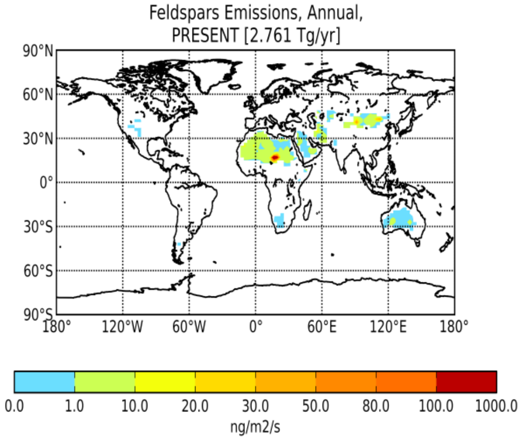

Feldspars Emissions, Annual, PRESENT [2.761 Tg/yr]

f)

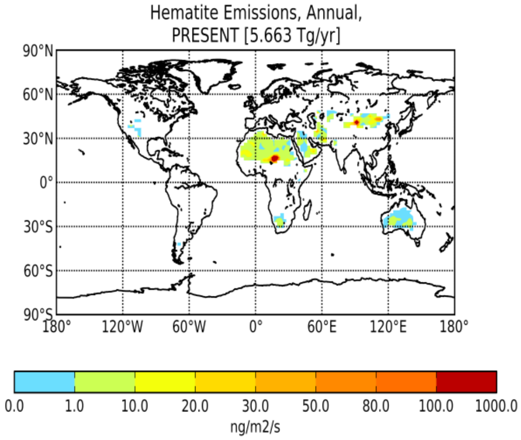

Hematite Emissions, Annual, PRESENT [5.663 Tg/yr]

g)

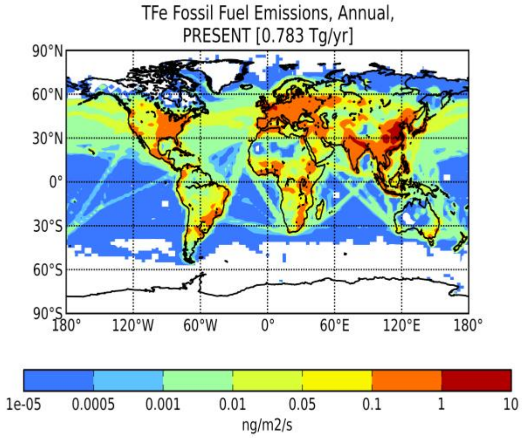

TFe Fossil Fuel Emissions, Annual, PRESENT [0.783 Tg/yr]

h)

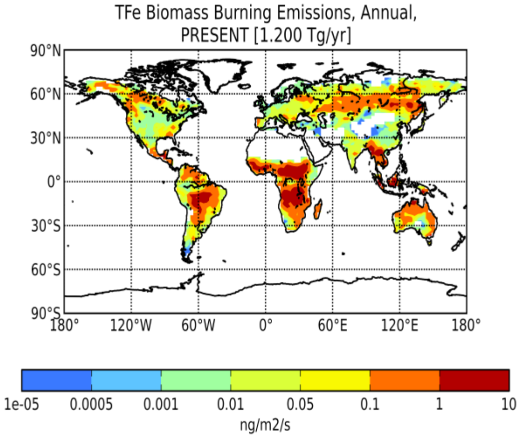

TFe Biomass Burning Emissions, Annual, PRESENT [1.200 Tg/yr]

Figure S2. pH values as calculated by TM4-ECPL for surface aerosol water for fine (a) and coarse (b) particles and for cloud water at 850hPa pressure level (c) and zonal mean (d) and the corresponding percentage changes (%) using PAST (left panels: e, g, i) and FUTURE (right panels: f, h, j) emissions with respect to the present-day (PRESENT) simulations.

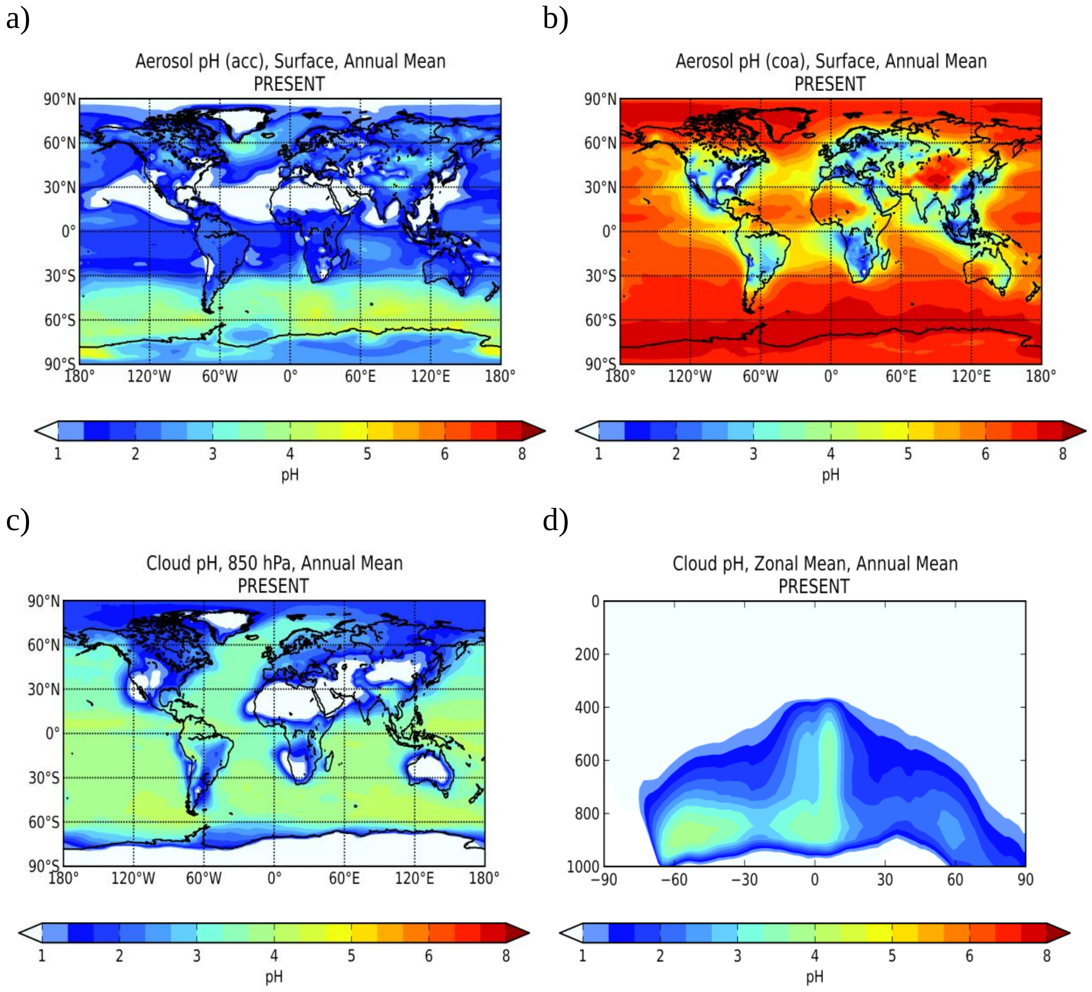

e)

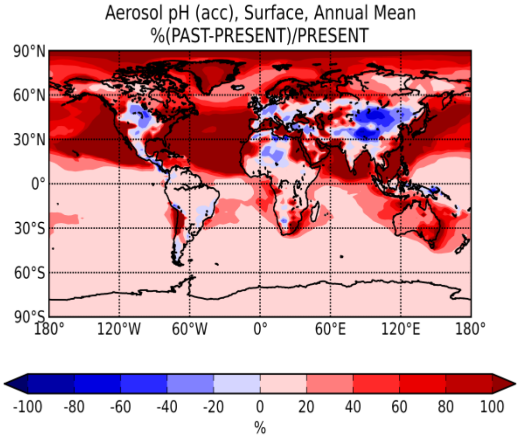
Aerosol pH (acc), Surface, Annual Mean
%(PAST-PRESENT)/PRESENT
90°N
60°N
30°N
0°
30°S
60°S
90°S
180°
120°W
60°W
0°
60°E
120°E
180°
-100
-80
-60
-40
-20
0
20
40
60
80
100
%

f)

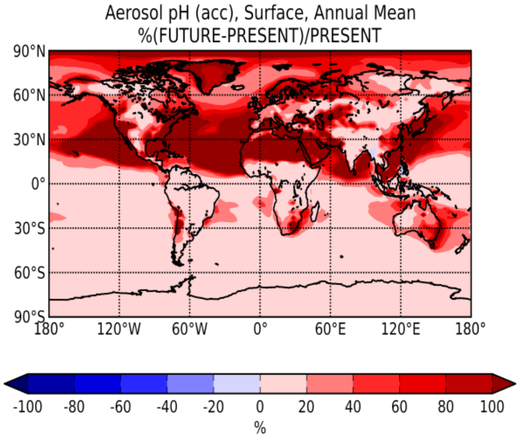
Aerosol pH (acc), Surface, Annual Mean
%(FUTURE-PRESENT)/PRESENT
90°N
60°N
30°N
0°
30°S
60°S
90°S
180°
120°W
60°W
0°
60°E
120°E
180°
-100
-80
-60
-40
-20
0
20
40
60
80
100
%

g)

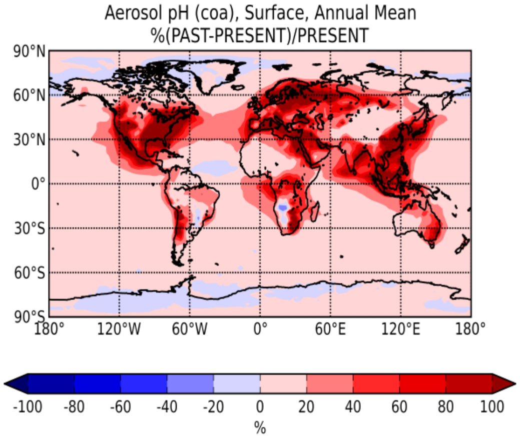
Aerosol pH (coa), Surface, Annual Mean
%(PAST-PRESENT)/PRESENT
90°N
60°N
30°N
0°
30°S
60°S
90°S
180°
120°W
60°W
0°
60°E
120°E
180°
-100
-80
-60
-40
-20
0
20
40
60
80
100
%

h)

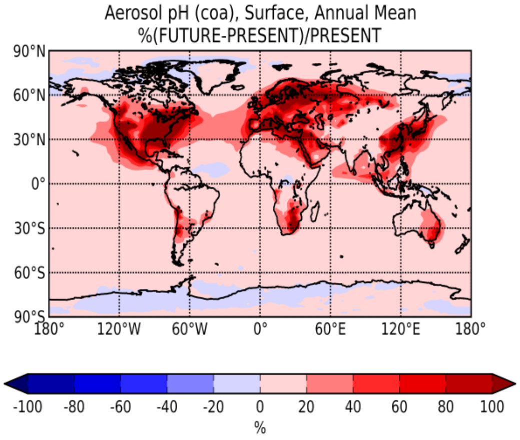
Aerosol pH (coa), Surface, Annual Mean
%(FUTURE-PRESENT)/PRESENT
90°N
60°N
30°N
0°
30°S
60°S
90°S
180°
120°W
60°W
0°
60°E
120°E
180°
-100
-80
-60
-40
-20
0
20
40
60
80
100
%

i)

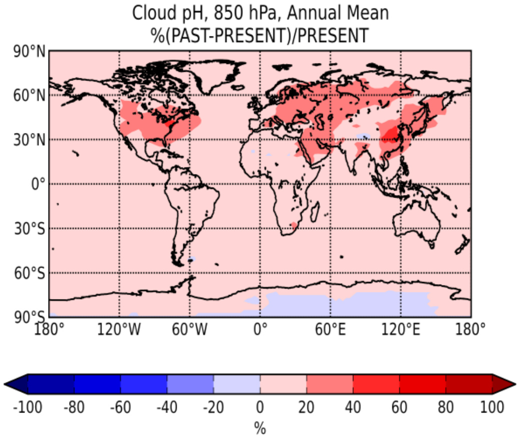
Cloud pH, 850 hPa, Annual Mean
%(PAST-PRESENT)/PRESENT
90°N
60°N
30°N
0°
30°S
60°S
90°S
180°
120°W
60°W
0°
60°E
120°E
180°
-100
-80
-60
-40
-20
0
20
40
60
80
100
%

j)

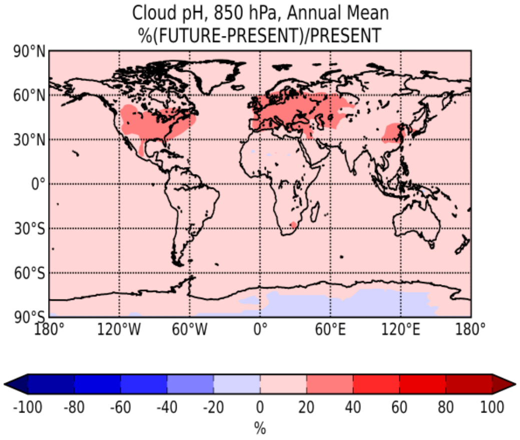
Cloud pH, 850 hPa, Annual Mean
%(FUTURE-PRESENT)/PRESENT
90°N
60°N
30°N
0°
30°S
60°S
90°S
180°
120°W
60°W
0°
60°E
120°E
180°
-100
-80
-60
-40
-20
0
20
40
60
80
100
%

Figure S3. Comparison of OXL surface concentrations with (+) and without (o) taking into account Fe-oxalato complexes in the aqueous-phase chemical scheme for measurements (red colour for urban sites, green colour for rural sites and blue colour for marine sites) as compiled by Myriokefalitakis et al. (2011).

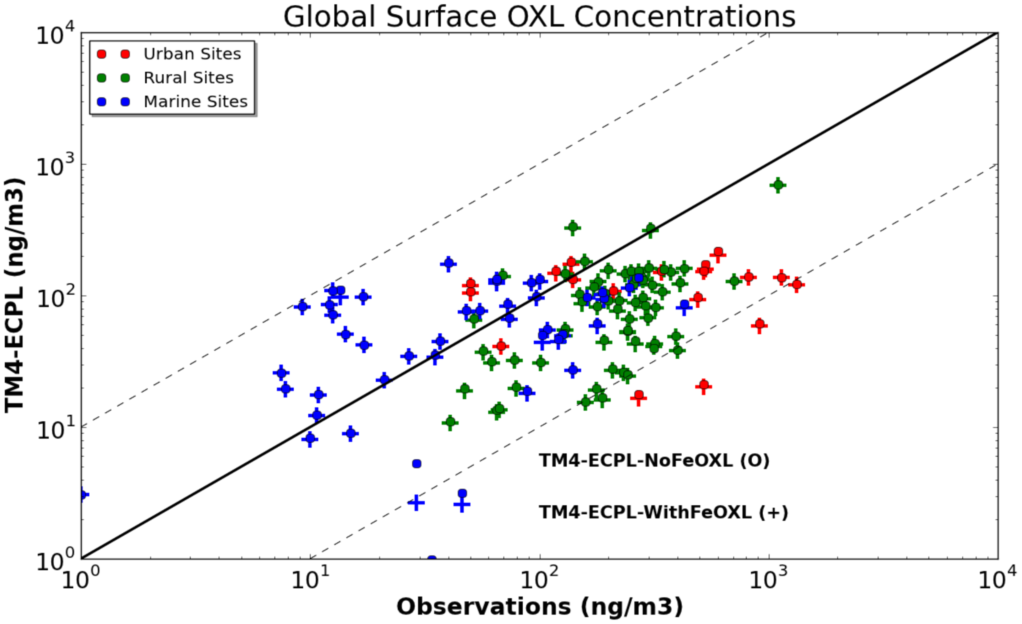

Figure S4. The percentage (%) iron solubility (SFe) predicted by the box model using the same chemical scheme with the global model, for dust concentrations 1 mg L^{-1} (assuming at time = 0 h initial SFe equals to zero), constant pH values of 1.5 (green line), 4.5 (blue line) and 8.5 (red line) and for initial (time = 0 h) oxalic acid (OXL) concentrations of a,b,c) 0 μM, d,e,f) 4.5 μM and g,h,i) 8 μM. Left column shows SFe=100x(Fe(II)+Fe(III))/TFe, middle column shows SFe(II)=100xFe(II)/TFe, right column shows SFe(III)=100xFe(III)/TFe.

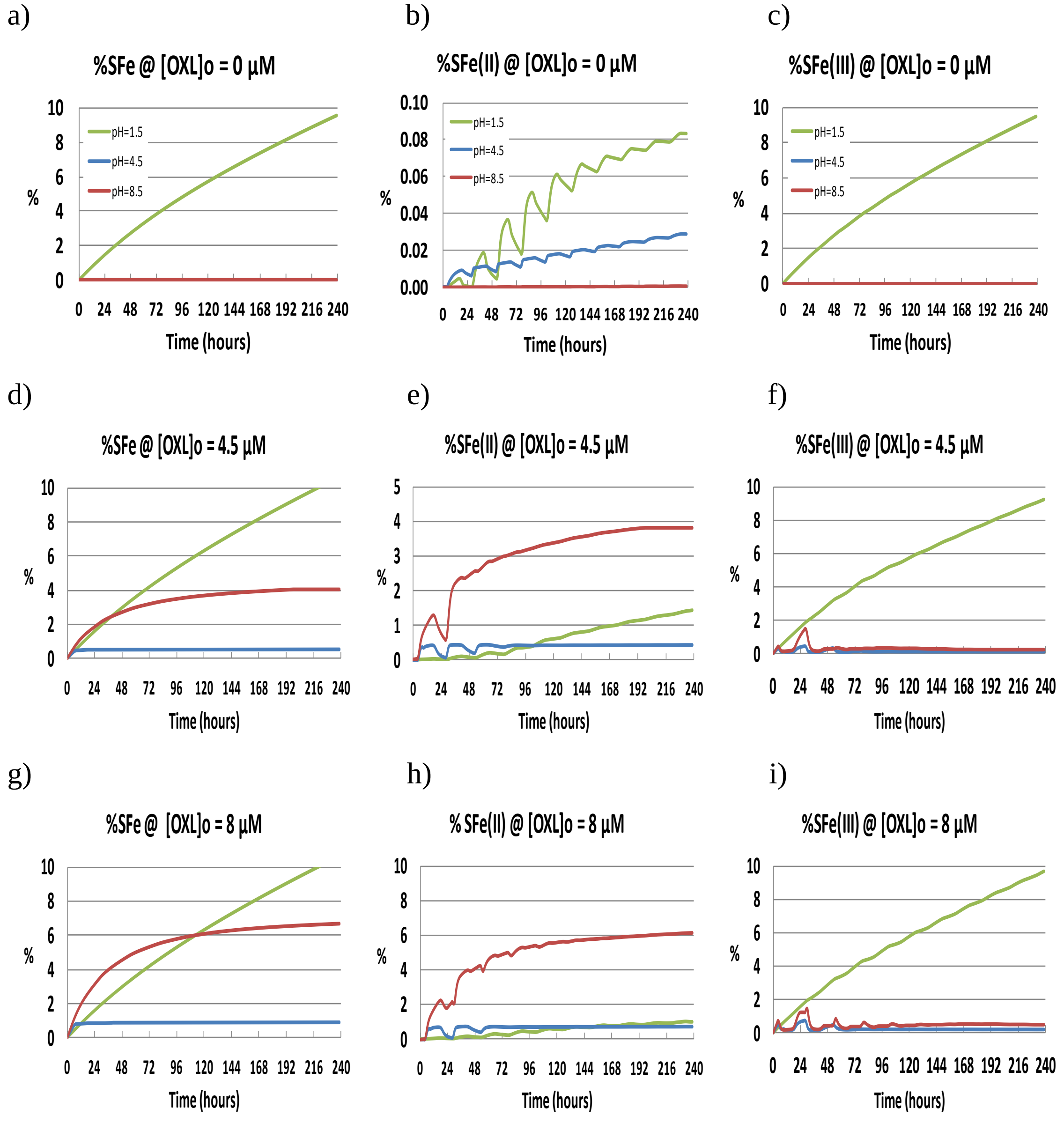

Figure S5. Calculated annual mean concentrations for the present atmosphere (in ng-Fe m^{-3}) for Fe(III) (sum of Fe^{3+} and ferric-oxalato complexes) (a,b) and Fe(II) (sum of Fe^{2+} and ferrous-oxalato complexes) (c,d) for surface (left panels; a,c) and zonal mean up to ~200 hPa (right panels; b,d). Note difference in scales.

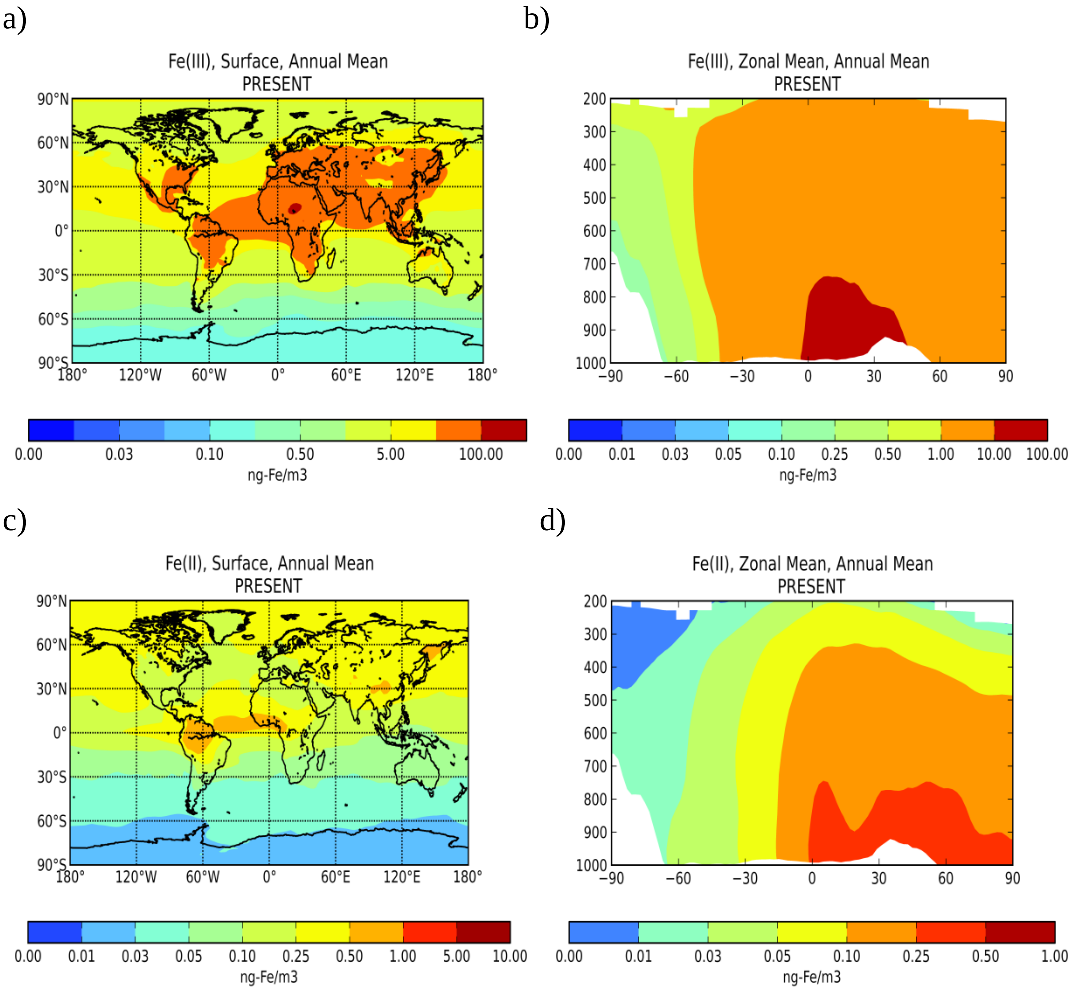

Figure S6. Annual mean Iron Solubility (SFe) calculated for the present atmosphere for a) all Fe sources; b) SFe in dust; c) SFe due to fossil fuel combustion emissions and d) SFe due to biomass burning emissions.

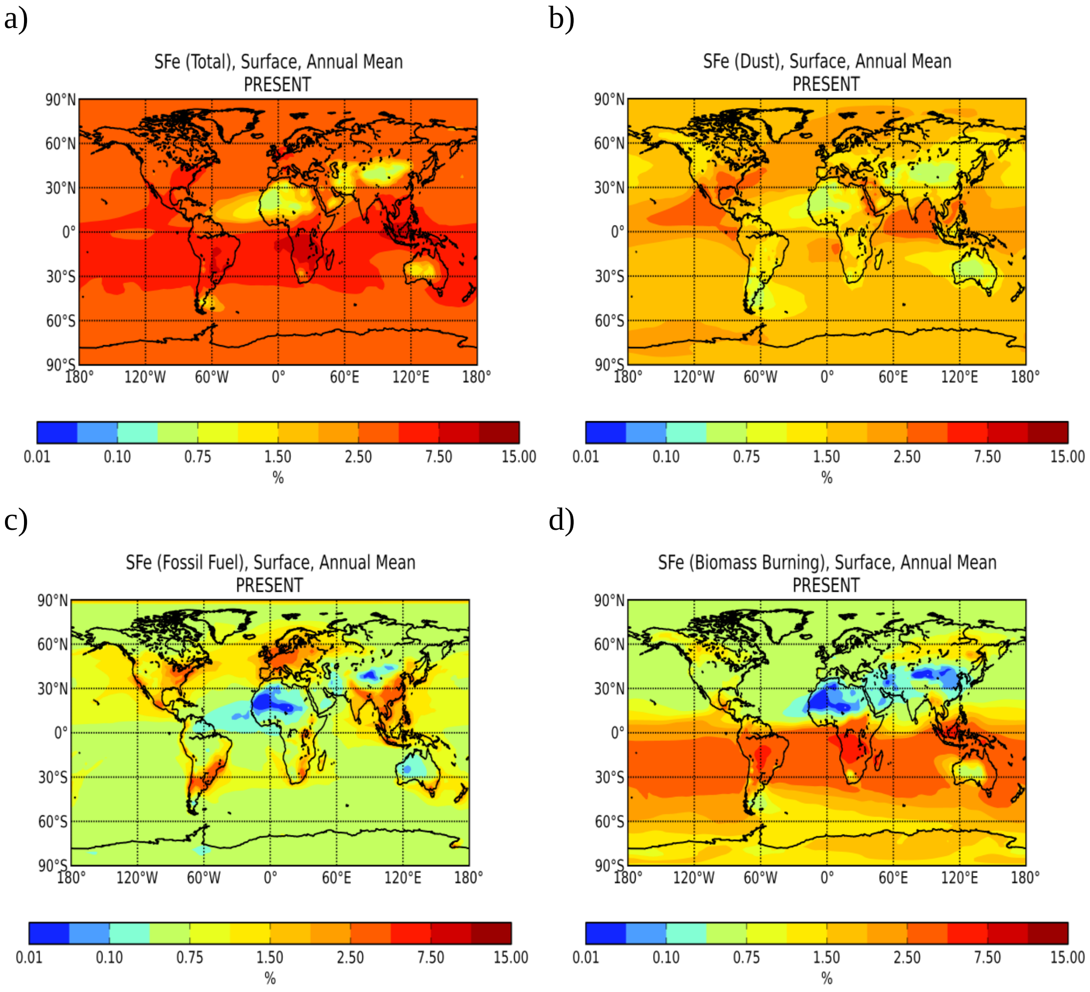

Figure S7. Oceanic regions (red colour) used for a-d) Fig. 7 deposition calculations (as described by Baker et al. 2013) and e) HNLC regions used for the Fig. 9 calculations, see text for definition.

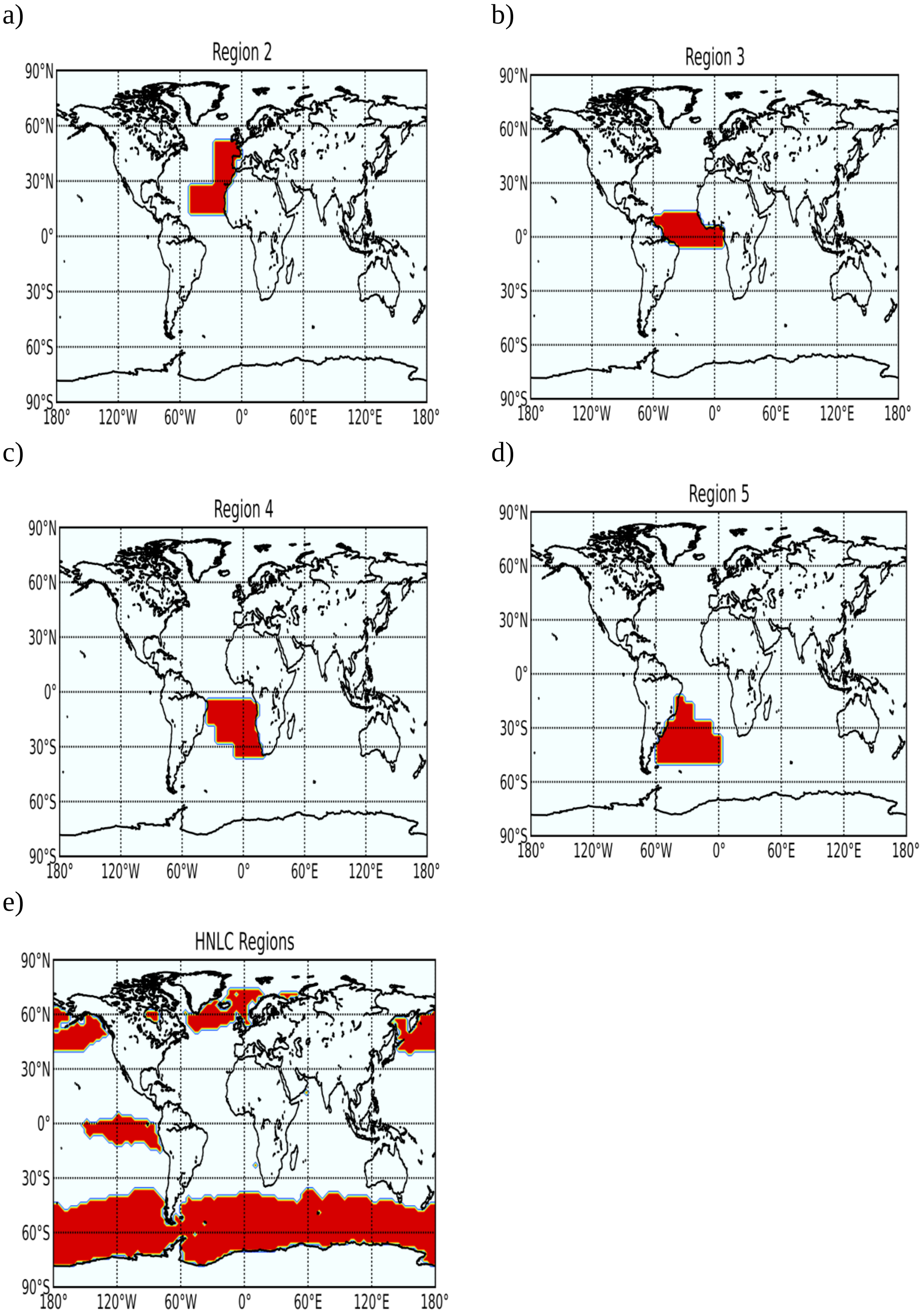

Figure S8. Absolute differences (in µg m^{-3}) of surface concentrations calculated by TM4-ECPL using the emissions of PAST (left panels: a, c, e, g) and FUTURE (right panels: b, d, f, h) from those calculated using the present-day emission scenario (PRESENT) for a, b) SO_4^{2-}; c, d) NH_4^+; e, f) NO_3^-; g, h) for OXL.

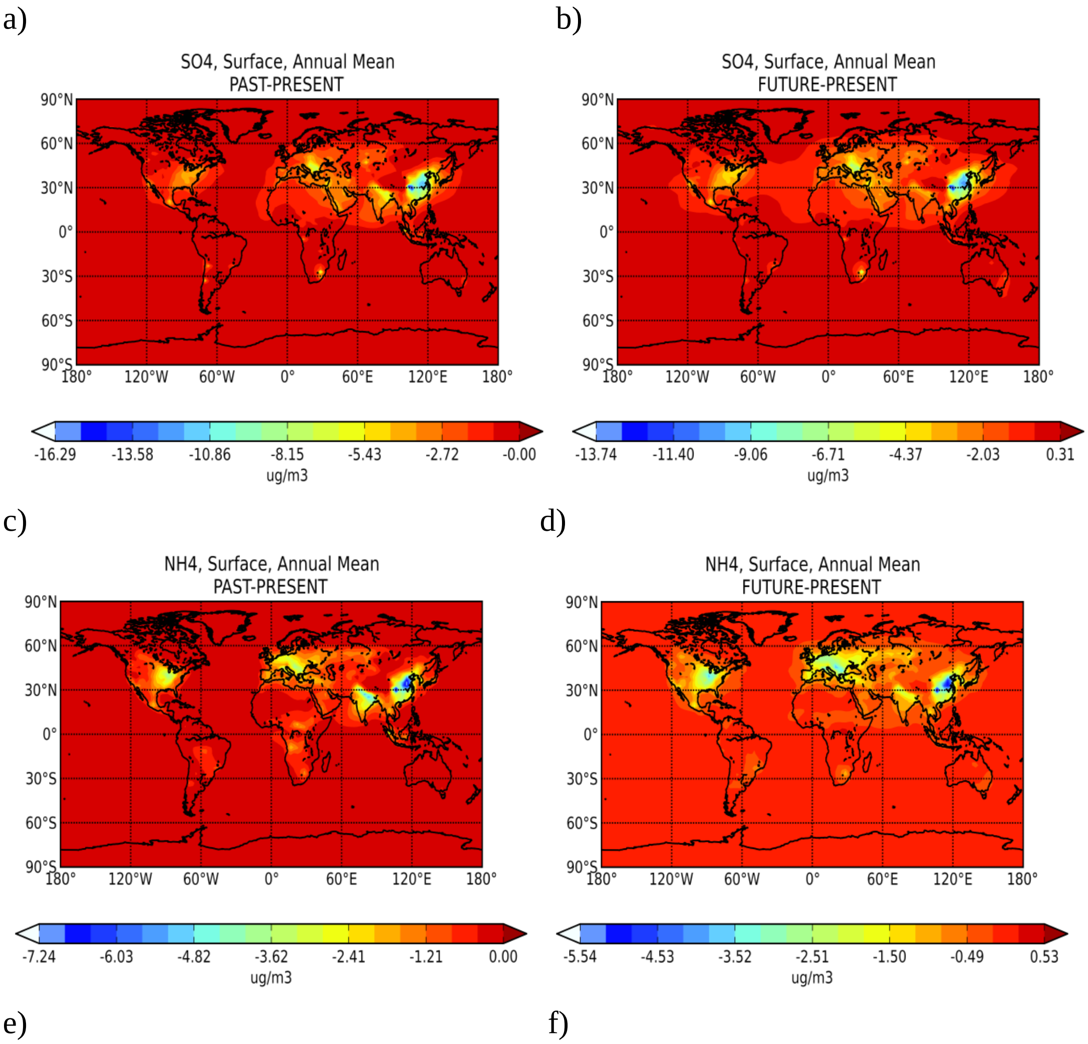

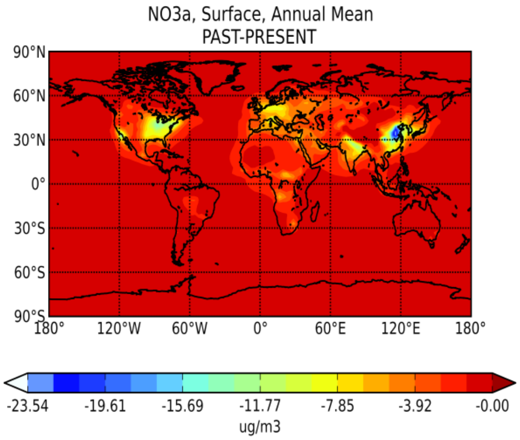
NO3a, Surface, Annual Mean
PAST-PRESENT
90°N
60°N
30°N
0°
30°S
60°S
90°S
180°
120°W
60°W
0°
60°E
120°E
180°
-23.54
-19.61
-15.69
-11.77
-7.85
-3.92
-0.00
ug/m3

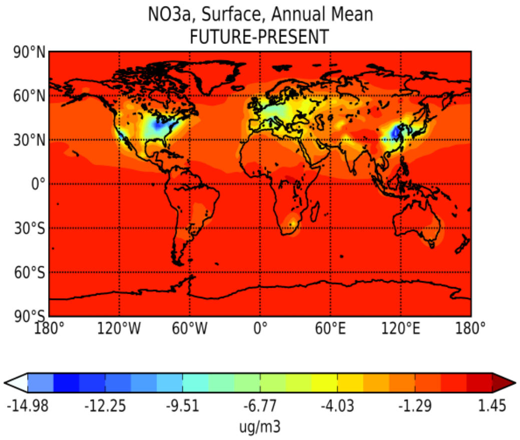
NO3a, Surface, Annual Mean
FUTURE-PRESENT
90°N
60°N
30°N
0°
30°S
60°S
90°S
180°
120°W
60°W
0°
60°E
120°E
180°
-14.98
-12.25
-9.51
-6.77
-4.03
-1.29
1.45
ug/m3

g)

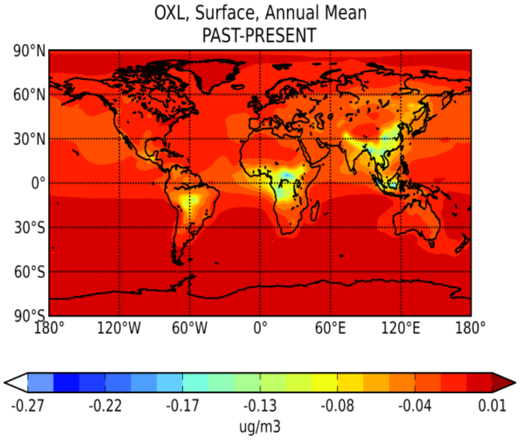
OXL, Surface, Annual Mean
PAST-PRESENT
90°N
60°N
30°N
0°
30°S
60°S
90°S
180°
120°W
60°W
0°
60°E
120°E
180°
-0.27
-0.22
-0.17
-0.13
-0.08
-0.04
0.01
ug/m3

h)

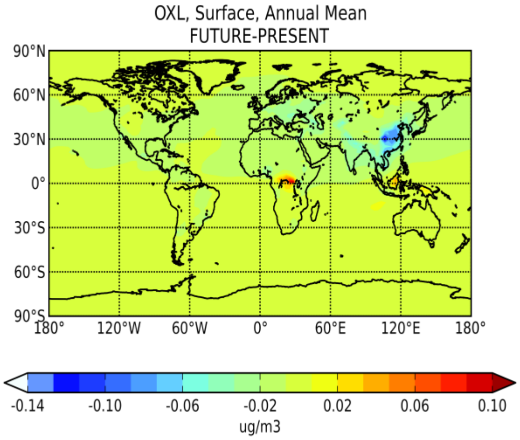
OXL, Surface, Annual Mean
FUTURE-PRESENT
90°N
60°N
30°N
0°
30°S
60°S
90°S
180°
120°W
60°W
0°
60°E
120°E
180°
-0.14
-0.10
-0.06
-0.02
0.02
0.06
0.10
ug/m3

Figure S9. Percentage differences (%) of PAST (left panels: a, c, f) and FUTURE (right panels: b, d, e) simulations from the PRESENT day simulation for annual mean surface concentrations of a, b) Fe(III); c, d) Fe(II) and e, f) DFe deposition as calculated by TM4-ECPL.

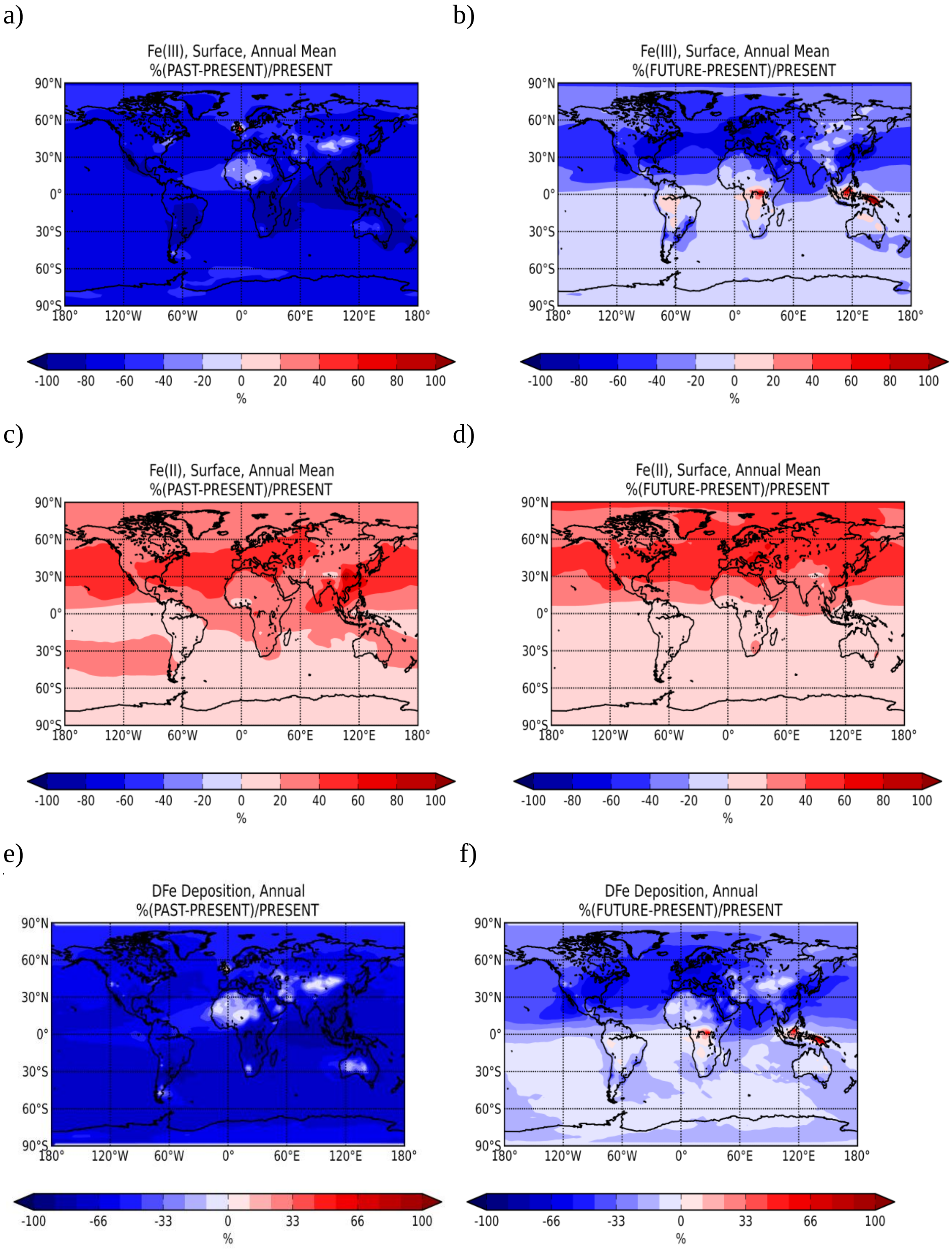

References

Benkelberg, H. J. and Warneck, P.: Photodecomposition of iron(III) hydroxo and sulfato complexes in aqueous solutions: Wavelength dependence of pH and SO −4 quantum yields, J. Phys. Chem., 99, 5214–5221, 1995.

Epstein, I. R., Kustin, K., and Simoyi, R. H.: Nitrous acid decomposition catalyzed by an iron(II) complex: Tris(3,4,7,8-tetramethyl-1,10-phenanthroline)iron(II)1 , J. Am. Chem. Soc., 104, 712–717, 1982.

Ervens, B., George, C., Williams, J. E., Buxton, G. V., Salmon, G. A., Bydde,r M., Wilkinson, F., Dentener, F., Mirabel, P., Wolk, R. and Herrmann, H. : CAPRAM 2.4 (MODAC mechanism): An extended and condensed tropospheric aqueous phase mechanism and its application, J. Geophys. Res., 108(D14), 4426, doi:10.1029/2002JD002202, 2003.

Jayson, G. G., Parson, B. J., and Swallow, A. J.: Oxidation of ferrous ions by perhydroxyl radicals, J. Chem. Soc. Faraday Trans., 69, 236–242, 1973.

Kremer, M. L.: The Fenton reaction, Dependence of the rate on pH, J. Phys. Chem. A, 107, 1734–1741, 2003.

Lin, G., Sillman, S., Penner, J. E. and Ito, A.: Global modeling of SOA: The use of different mechanisms for aqueous-phase formation, Atmos. Chem. Phys., 14, 5451–5475, doi:10.5194/acp-14-5451-2014, 2014.

Logager, T., Holcman, J., Sehested, K., and Pedersen, T.: Oxidation of ferrous ions by ozone in acidic solution, Inorg. Chem., 31, 3523–3529, 1992.

Pikaev, A. K., Sibirskaya, G. K., Shirshov, E. M., Glazunov, P. Y., and Spitsyn, V. I.: Pulsed radiolysis of concentrated aqueous solutions of nitric acid, Dokl. Phys. Chem., Proc. Acad. Sci. USSR, 215, 328–331, 1974.

Rush, J. D. and Bielski, B. H. J.: Pulse radiolytic studies of the reactions of HO2/O2 with Fe(II)/Fe(III) ions, The reactivity of HO2/O2 with ferric ions and its implication on the occurrence of the Haber-Weiss reaction, J. Phys. Chem., 89, 5062–5066, doi:10.1021/j100269a035, 1985.

Rush, J. D. and Bielski, B. H. J.: Pulse radiolytic studies of thereactions of HO2/O2 with Fe(II)/Fe(III) ions, The reactivity of HO2/O2 with ferric ions and its implication on the occurrence of the Haber-Weiss reaction, J. Phys. Chem., 89, 5062–5066, doi:10.1021/j100269a035, 1985.

Sedlak, D. L. and Hoigne, J.: The role of copper and oxalate in the´ redox cycling of iron in atmospheric waters, Atmos. Environ., 27A, 2173–2185, 1993.